

Self-Consistent, Integrated, Advanced Tokamak Operation in DIII-D*

M.R. Wade,¹ M. Murakami,¹ T.A. Casper,² J.R. Ferron,³ A.M. Garofalo,⁴ C.M. Greenfield,³ A.W. Hyatt,³ R. Jayakumar,² J.E. Kinsey,⁵ L.L. Lao,³ J. Lohr,³ T.C. Luce,³ M.A. Makowski,² C.C. Petty,³ P.A. Politzer,³ R. Prater,³ and W.P. West³

¹Oak Ridge National Laboratory, Oak Ridge, Tennessee, 37831 USA
email: wade@fusion.gat.com

²Lawrence Livermore National Laboratory, Livermore, California 94551 USA

³General Atomics, P.O. Box 85608, San Diego, California, 92186-5608 USA

⁴Columbia University, New York

⁵Lehigh University, Bethlehem, Pennsylvania 18015 USA

Recent experiments on DIII-D have demonstrated the ability to sustain plasma conditions that self consistently integrate and sustain the key ingredients of Advanced Tokamak (AT) operation: high β at high q_{\min} , good plasma confinement with $H_{99} \sim 2.5$, and high current drive efficiency. Utilizing off-axis ($\rho = 0.4$) ECCD to modify the current density profile in a plasma operating near the no-wall ideal stability limit with $q_{\min} > 2.0$, plasmas with $\beta \sim 2.9\%$ and 90% of the plasma current driven non-inductively are produced and sustained for nearly 2 s (limited only by the duration of the ECCD pulse). While many experiments worldwide (including many done on DIII-D) have demonstrated the key components individually, this is the first experiment to self consistently integrate these elements simultaneously. In these discharges, ECCD is integral in producing negative central magnetic shear, helping to form a weak internal transport barrier (for both ions and electrons) that is maintained in the presence of a fully developed H-mode edge with Type I ELMs. This is in distinct contrast to typical observation of significant confinement deterioration when using ECH/ECCD in plasmas with $T_i/T_e \gg 1$.

Figure 1 shows the temporal evolution of a representative shot of this class of discharges. Early in the current ramp, an H-mode is induced to slow down the penetration of the current density in order to achieve $q_{\min} > 2.5$ at the end of the current ramp. Subsequently, β_N is increased and then maintained at ~ 2.8 for the remainder of the discharge through feedback control of the neutral beam injection (NBI). At 1.5 s, approximately 2.5 MW of ECCD is applied with the resonance location at $\rho = 0.4$ near the inboard midplane. A large increase in negative magnetic shear is produced within 500 ms of the initiation of ECCD and then maintained for the duration of the ECCD pulse (1.3 s) with q_0 increasing to above 4.0 while q_{\min} remains above 2.0. Comparisons to cases with radially launched ECH (therefore no

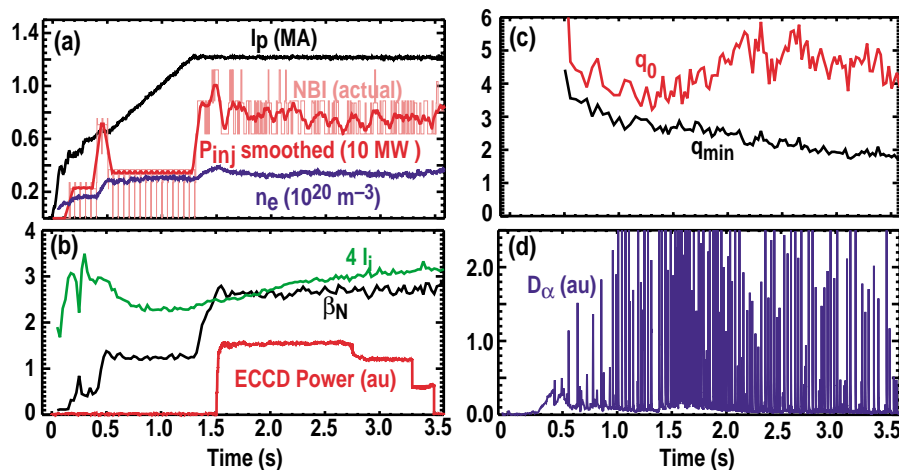


Fig. 1. Plasma parameters versus time for AT discharge #111203 exhibiting strong negative central shear and an internal transport barrier for nearly 2.0 s: (a) plasma current (MA), neutral beam injected power ($\times 10$ MW) and line-averaged density ($\times 10^{20} \text{ m}^{-3}$) (b) β_N , $4 l_I$ and ECCD power; (c) q_0 and q_{\min} , and (d) D_α (a.u.).

*Work supported by U.S. Department of Energy under Contracts DE-AC05-00OR22725, W-7405-ENG-48, DE-AC03-99ER54463, and Grants DE-FG02-89ER53297, and DE-FG02-92ER54141.

current drive) indicate that the current profile modification is almost entirely due to ECCD as the ECH case shows little difference from an NBI-only case. This result is not unique as clear modifications of the current profile have also been observed in other types of AT plasmas including QDB discharges. In the present case, analysis indicates that approximately 130 kA of current is generated from ECCD ($\sim 10\%$ of the total current). This value is consistent with theoretical predictions using the Fokker-Planck code CQL3D. The ECCD efficiency is favorably affected by the high field side resonance location (reduced electron trapping) and operation at high β_e which enhances absorption by electrons far from the trapping boundary. The remainder of the plasma current is provided by neutral beam current drive ($\sim 30\%$), the bootstrap current ($\sim 50\%$) and Ohmic current ($\sim 10\%$).

Coincident with the changes in the magnetic shear in the core, improvements are observed in the particle, electron energy, ion energy and momentum transport. These improvements lead to increases in both the electron and ion temperature as well as electron density and toroidal rotation velocity (Fig. 2). Weak transport barriers are evident in the ion temperature and toroidal rotation profiles with the foot of the barrier being near the shear reversal region. Since the primary difference between the ECCD case and the other cases is the evolution of the current density profile, it is believed that these improved transport properties result primarily from the increase in negative magnetic shear induced by the ECCD. Preliminary analysis using the GKS gyro-kinetic code indicates that both negative magnetic shear and $E \times B$ shear are stabilizing in this case. The former is particularly important for electron transport since magnetic shear stabilization reduces turbulence growth rates over a wide range of turbulence scale lengths, in contrast to $E \times B$ shear, which primarily affects long-wavelength turbulence.

The observed evolution in current density profile is nearly identical to that predicted by simulations carried out prior to the experiment. These simulations use a suite of transport codes combined with an ECCD ray-tracing code to self-consistently simulate the radial transport of energy and current based on experimentally observed transport properties. Simulations based on the present experimental data indicate that a modest increase in ECCD power (from 2.5 to 3.5 MW) distributed broadly off-axis ($\Delta_{FWHM}=0.27$ centered at $\rho_{EC}=0.38$) should be able to maintain a favorable current density profile for the duration of ECCD pulse. Studies of the sensitivity of these results to the prescribed transport coefficients have shown that the favorable q profile can be maintained even if χ_e and χ_i are increased by a factor of 2 for $\rho \leq 0.8$ over the base case.

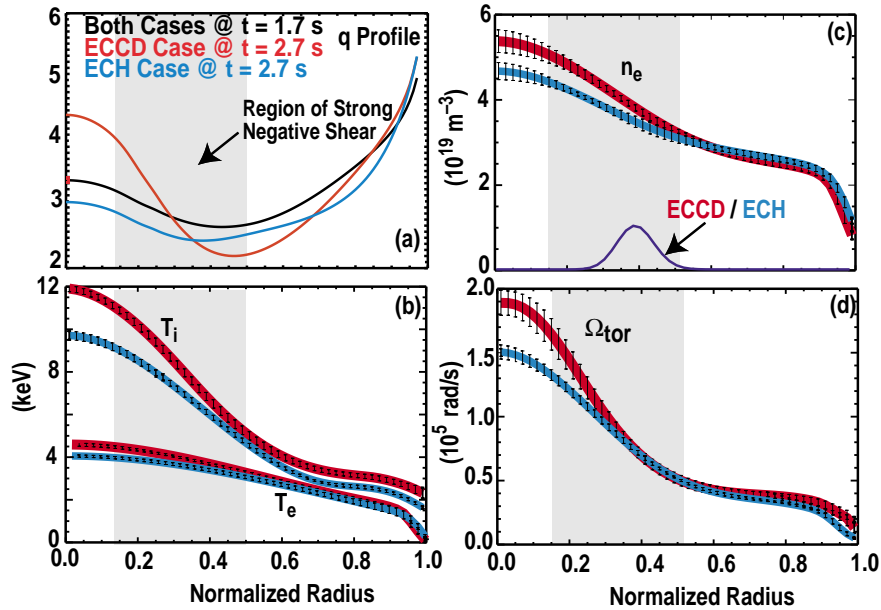


Fig. 2. Radial profiles of (a) safety factor, (b) ion and electron temperature, (c) electron density; and (d) toroidal angular velocity for discharges ECCD + NBI (red) and ECH + NBI (blue). The error bars are based on the variation of the fitted profiles over 300 ms (12 fits).